Journal of Catalysis **208,** 345–358 (2002)
doi:10.1006/jcat.2002.3602

1,1- and 1,3-Diiodo Neopentanes on Pt(111): Intermediates during Hydrocarbon Catalytic Conversion Reactions

Ton V. W. Janssens[1] and Francisco Zaera[2]

Department of Chemistry, University of California, Riverside, California 92521

Received October 10, 2001; revised March 13, 2002; accepted March 13, 2002

The chemistry of 1,1- and 1,3-diiodo neopentanes, precursors to neopentylidene and 2,2-dimethyl propane-1,3-diyl intermediates, respectively, was probed on a Pt(111) single-crystal surface by temperature-programmed desorption (TPD) and reflection–adsorption infrared spectroscopy (RAIRS). The sequential surface activation of the two C–I bonds in those compounds is manifested by the formation of neopentyl iodide and neopentane in TPD experiments. Dosing of the 1,3-diiodo compound at 230 K leads to the formation of the expected cyclic 2,2-dimethyl propane-1,3-diyl intermediate, with the main ring perpendicular to the surface. Activation of the 1,1-isomer, on the other hand, leads to the formation of 2,2-dimethyl propane-1-yl-3-ylidene, presumably via γ-H elimination from neopentylidene. The surface species that result from 1,1-diiodo neopentane are more reactive and dehydrogenate to a larger extent than those from the 1,3-diiodo analog, but both eventually convert to neopentylidyne. The implications of this chemistry to hydrocarbon catalytic processes such as oil reforming are discussed.

1. INTRODUCTION

The catalytic conversion of hydrocarbons on transition-metal surfaces involves a number of difficult to isolate intermediates. One approach for the study of the surface chemistry of such intermediates, developed in our laboratory and widely employed nowadays by other surface-science research groups, is the use of halo hydrocarbon precursors (1–9). It has been shown that the carbon–halogen bonds in adsorbed halo hydrocarbons (carbon–iodine bonds in particular) are quite labile and can be easily activated thermally or photolytically to produce the corresponding hydrocarbon species (10–13). The versatility of this procedure has allowed the initial work on alkyl groups (14–28) to be extended to the production of surface carbenes (29–32), vinyls (33, 34), allyls (35–38), metallacycles (39–43), and oxametallacycles (44, 45).

Understanding the nature of the hydrocarbon species that form on the surface during catalysis is of particular importance for the design of more-selective reforming processes (6, 46–50). From the mechanistic point of view, past studies by us have pointed to the preference for dehydrogenation of hydrocarbon surface species at the β (second from the surface) carbon (51), the same as in organometallic compounds (4). That step is in fact the one responsible for the rapid equilibrium between alkanes and alkenes under most reforming conditions. However, it has also become clear that hydrogen elimination at other positions in the hydrocarbon chain are required for the promotion of isomerization, cyclization, and hydrogenolysis reactions (52–54). It is our contention that the selectivity of reforming reactions is controlled mainly by the regioselectivity of the first dehydrogenation step from alkyl surface intermediates (8, 9, 39, 55, 56). One way to test this hypothesis is to study the surface chemistry of hydrocarbon species such as neopentyl moieties, which lack hydrogen atoms at the β position.

Most of our work on the surface chemistry of neopentyl iodide on Ni(100) (39, 57, 58) and Pt(111) (59–61) has been published previously. It was found that, on nickel, dehydrogenation occurs preferentially at the α position: the resulting neopentylidene species forms below 150 K and decomposes via C_α–C_β bond scission to produce isobutene above 350 K (58). On platinum, by contrast, α- and γ-H eliminations display comparable rates (59, 61). Infrared spectroscopy data suggest that those two reactions lead to the formation of the expected neopentylidene and 2,2-dimethyl propane-1,3-diyl intermediates, respectively (60). Here we present results from our studies with 1,1- and 1,3-diiodo neopentanes to expand on the detailing of the chemistry of those intermediates. The overall reaction scheme derived from this work is presented in Fig. 10.

2. EXPERIMENTAL

The experiments reported here were performed in an ultrahigh vacuum (UHV) chamber cryopumped to a base pressure below 1×10^{-10} Torr and equipped with an ion gun for sputtering of the surface, a UTI-100C quadrupole

[1] Present address: Haldor Topsøe A/S, P.O. Box 213, Nymøllevej 55, DK-2800 Lyngby, Denmark.

[2] To whom correspondence should be addressed. Fax: 1 (909) 787-3962. E-mail: francisco.zaera@ucr.edu.

0021-9517/02 $35.00

mass spectrometer for temperature-programmed desorption (TPD), and a Fourier transform infrared spectrometer for reflection–absorption infrared spectroscopy (RAIRS), as described elsewhere (38, 62). Briefly, the UTI mass spectrometer is connected to a personal computer in an arrangement that allows for data collection of up to 15 masses simultaneously in a TPD single experiment. Its ionizer is covered with a cone having a front hole about 4 mm in diameter which can be placed at less than a millimeter from the surface in order to enhance the selective detection of the desorbing products. The TPD spectra are reported in arbitrary units, but relative scales are provided for comparison. The Pt(111) single crystal was mounted on a sample holder capable of cooling to 100 K and of resistive heating to above 1000 K. The temperature was measured with a chromel–alumel thermocouple spot welded to the back of the crystal. Linear temperature ramps of 10.0 ± 0.5 K/s were used in all the TPD experiments by using a homemade temperature controller.

The RAIRS experiments were performed by focusing the IR beam from a Mattson Sirius 100 FTIR spectrometer through a sodium chloride window onto the sample inside the UHV chamber, and by picking up the reflected beam, passing it through a second sodium chloride window and a polarizer, and collecting it with a mercury–cadmium–telluride (MCT) detector. Grazing incidence was used to optimize the signal from the surface species. Data from either 1000 or 2000 scans, taken with 4-cm^{-1} resolution, were averaged and ratioed against spectra from the clean surface recorded immediately before dosing. All the RAIRS data were taken at sample temperatures below 130 K.

The sample was routinely cleaned by cycles of sputtering with Ar^+ ions at room temperature, oxidation in 3×10^{-7} Torr oxygen at 700 K, and annealing in vacuum at 1000 K. Gas doses are reported in Langmuirs ($1\ \mathrm{L} = 1 \times 10^{-6}$ Torr · s), uncorrected for differences in ion gauge sensitivity. The 1,1-diiodo-2,2-dimethyl propane (98% purity) was purchased from Aldrich and used without further treatment other than a series of freeze-pump-thaw cycles before introduction into the UHV chamber. The 1,3-diiodo-2,2-dimethyl propane was prepared via iodine substitution of neopentyl glycol (Aldrich, 99%) with methyl iodide (63). The hydrogen (99.99%) and deuterium (>99.5% isotopic purity) used in the coadsorption experiments were obtained from Matheson and used as supplied.

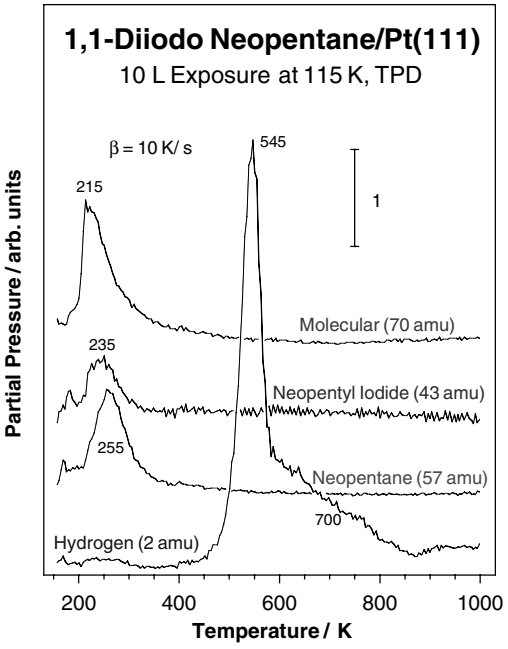

FIG. 1. Temperature-programmed desorption (TPD) spectra from 10 L of 1,1-diiodo neopentane dosed on a Pt(111) single-crystal surface at 115 K. Traces are shown for 2 (hydrogen), 43 (neopentyl iodide), 57 (neopentane), and 70 (diiodo neopentane) amu, but many other masses were probed to corroborate our assignment. A linear heating rate of 10 K/s was used in all experiments. The sequential scission of the C–I bonds is inferred by the production of neopentyl iodide and neopentane. The resulting surface species dehydrogenate to surface carbon between 500 and 800 K.

3. RESULTS

3.1. 1,1- and 1,3-Diido Neopentane TPD on Clean Pt(111)

Based on our previous knowledge of the surface chemistry of alkyl halides on metals (2, 31, 41, 42), 1,1- and 1,3-diiodo neopentanes were chosen in this study as potential precursors for the formation of neopentylidene and 2,2-dimethyl propane-1,3-diyl intermediates, respectively. Temperature-programmed desorption (TPD) experiments with each of those molecules adsorbed on clean Pt(111) at 115 K are reported first. Results from an experiment with 10 L of 1,1-diiodo neopentane are displayed in Fig. 1, while data from analogous experiment with the 1,3 isomer are reported in Fig. 2. As with neopentyl iodide (60), three main desorbing products were detected here, namely hydrogen (2 amu), neopentane (57 amu), and neopentyl iodide (43 or 71 amu); a number of other masses were used to corroborate these assignments. Most of the hydrogen desorbs above 400 K, indicating that extensive decomposition occurs at reasonably high temperatures, and that therefore at least one stable surface hydrocarbon intermediate should be isolatable in each case. In the case of the 1,1-diiodo compound, the first hydrogen TPD peak reaches its maximum at 545 K and is quite intense. With 1,3-diiodo neopentane, that feature peaks around 520 K, is much weaker, and is preceded by a shoulder at about 460 K. A broad, higher temperature (~700 K), tail is seen in both cases as well.

Neopentane desorbs in a single broad feature in both 1,1- and 1,3-diiodo neopentane, at about 255 and 285 K, respectively. This is approximately the same temperature range observed for neopentane production from neopentyl iodide thermal activation on clean Pt(111), suggesting similar

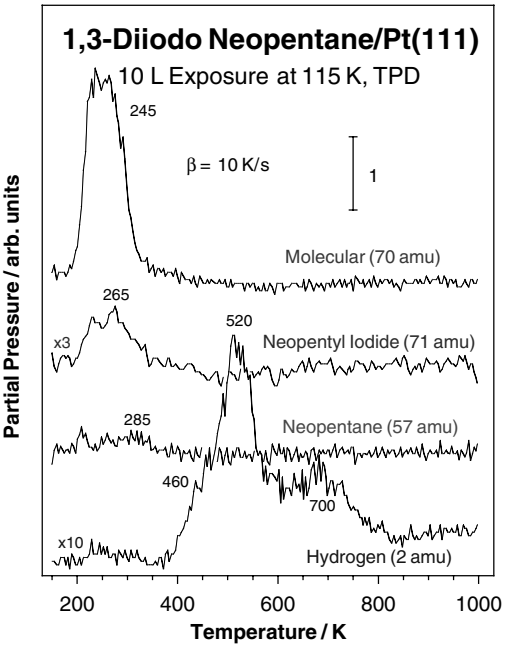

FIG. 2. TPD spectra from 10 L of 1,3-diiodo neopentane dosed on a Pt(111) single-crystal surface at 115 K. Traces are shown for 2 (hydrogen), 57 (neopentane), 71 (neopentyl iodide), and 70 (diiodo neopentane) amu. The sequential scission of the C–I bonds is again indicated by the production of neopentyl iodide and neopentane, but much less decomposition of surface species is seen here as compared to the case of the 1,1-diiodo compound in Fig. 1.

chemistry in all three cases (60). Neopentyl iodide desorption is detected at a somewhat lower temperatures, around 235 and 265 K, respectively, indicating sequential C–I bond scission steps and easy hydrogenation of the monoiodo surface intermediate. Significant amounts of molecular desorption were detected for both compounds as well, at 215 and 245 K, respectively. Notice that the relative trends in temperature maxima for the different hydrocarbon products from the two diiodo neopentanes are similar.

In terms of yields, it is clear that a larger fraction of the 1,1-diiodo compound decomposes on Pt(111) as compared to the 1,3-diiodo case. A quantitative analysis of the data (based on the TPD areas, corrected for relative sensitivities from independent control mass spectra) bares this out: only about 20% of the adsorbed 1,3-diiodo neopentane decomposes on the surface, compared to approximately half of the 1,1-isomer. Also, from those reacting fractions, about half (26%) undergo total dehydrogenation in the first system, but only 2% does so in the second. It is interesting that only less than 4% of the adsorbed 1,1-diiodo neopentane desorbs as neopentyl iodide; 20% is detected in the form of neopentane. In contrast, the neopentyl iodide : neopentane ratio is significantly larger (12% : 9%) with 1,3-diiodo neopentane. Clearly, the initial monoiodo intermediate from 1,1-diiodo neopentane (presumably 1-iodo neopentyl, Pt_n–$CHIC(CH_3)_3$) can react at a much faster rate than that from the 1,3-diiodo compound (a 3-iodo neopentyl, Pt_n–$CH_2C(CH_3)_2CH_2I$, counterpart).

Figure 3 shows TPD traces for the minority products seen in the TPD experiments reported above. A number of lighter hydrocarbons were indeed detected in small quantities in these studies, methane and isobutene in particular. Methane production is seen as a sharp peak about 165 K in the case of 1,1-diiodo neopentane, but no C_1 products are observed with 1,3-diiodo neopentane. On the other hand, isobutene production was detected in both cases, in a broad range between 140 and 200 K in the first case, and in a better defined feature about 210 K in the second. The unequivocal identification of other hydrocarbons could not be achieved with the data available from our studies, but their production is plausible.

3.2. Deuterium Coadsorption

Additional information on the surface chemistry of the C_5 compounds was obtained from TPD experiments with coadsorbed deuterium. The most relevant traces from surfaces dosed sequentially with 20 L of deuterium and 10 L of 1,1- or 1,3-diiodo neopentanes are reported in Figs. 4 and 5, respectively. Three panels are displayed in each figure, summarizing the data for hydrogen, neopentane, and neopentyl iodide and molecular desorption, respectively.

The use of D_2 in these experiments helps track the fate of the hydrogen atoms within the desorption products. Specifically, the traces in the left panels of Figs. 4 and 5 clearly differentiate between the predominant deuterium signal originating from D_2 predosing (the signals about 255 and

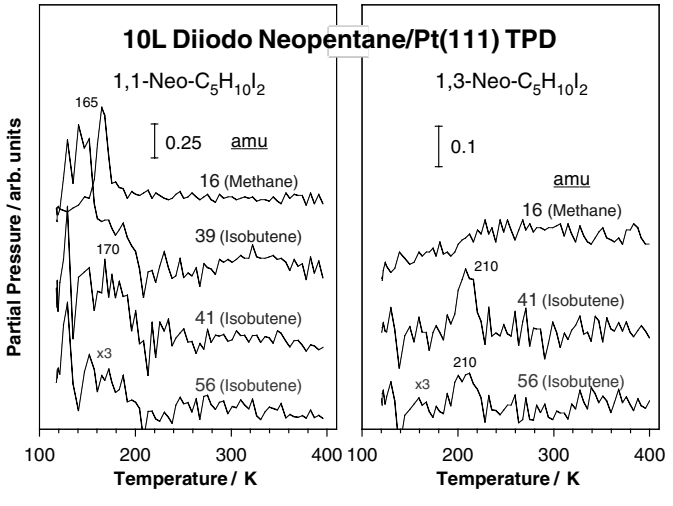

FIG. 3. Additional TPD spectra from 10 L of 1,1- (left) and 1,3- (right) diiodo neopentanes dosed on a Pt(111) single-crystal surface at 115 K. Shown here are the signals for some minor decomposition products, namely for 16 amu (methane) and for 39, 41, and 56 amu (isobutene). Isobutene production is seen in both cases, between 140 and 200 with 1,1-diiodo neopentane and around 210 K with the 1,3-diiodo isomer, but methane desorption is only observed with the former compound.

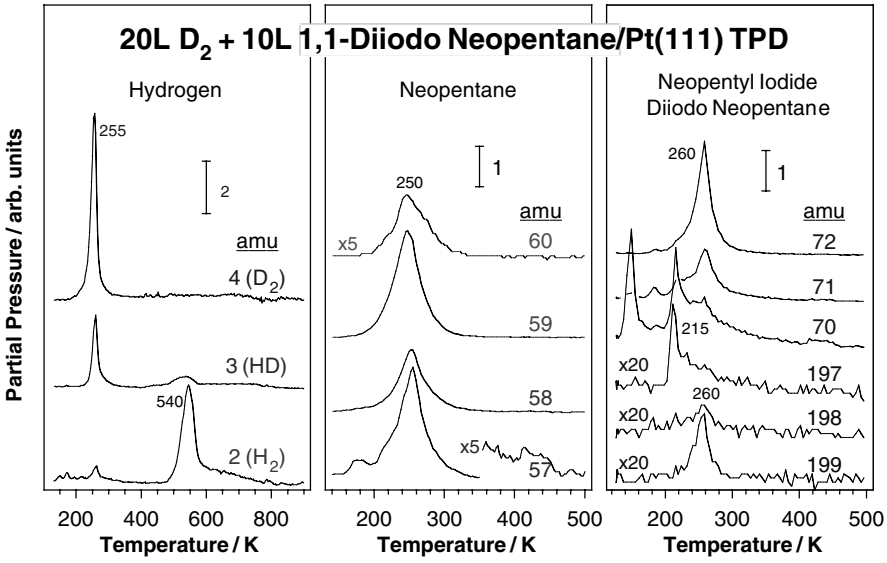

FIG. 4. Hydrogen (2 (H_2), 3 (HD), and 4 (D_2) amu, left panel), neopentane (57–60 amu, center), and neopentyl iodide and diiodo neopentane (70–71 and 197–199 amu, right) TPD spectra from a Pt(111) surface dosed at 110 K sequentially with 20 L of D_2 and 10 L of 1,1-diiodo neopentane. H–D exchange is manifested by the desorption of neopentane molecules with multiple deuterium substitutions, and extensive dehydrogenation is indicated by the high temperature peaks in the 2- and 3-amu traces.

270 K in the 3 (HD) and 4 (D_2) amu traces in the TPD spectra for 1,1- and 1,3-diiodo neopentane, respectively), and the normal hydrogen resulting from surface decomposition reactions (the peaks above 350 K in the 2 (H_2) and 3 (HD) amu data). It is clear that some diiodo neopentane decomposes even in the presence of coadsorbed deuterium, significantly more in the case of the 1,1-isomer. On the other hand, it is also evident that the extent of that decomposition is inhibited significantly, from 26 to 11% of the total surface species in the case of 1,1-diiodo neopentane, and from 2 to <1% with the 1,3-diiodo compound. Finally, the bulk of the decomposition of the surface intermediates formed around 300 K take place at much higher temperatures, above 500 K with 1,1-diiodo neopentane, and in a more stepwise manner at about 350, 510, and 660 K with the 1,3-diiodo compound. This attests to the great stability of the surface intermediate(s) produced by the initial decomposition of the diiodo neopentanes.

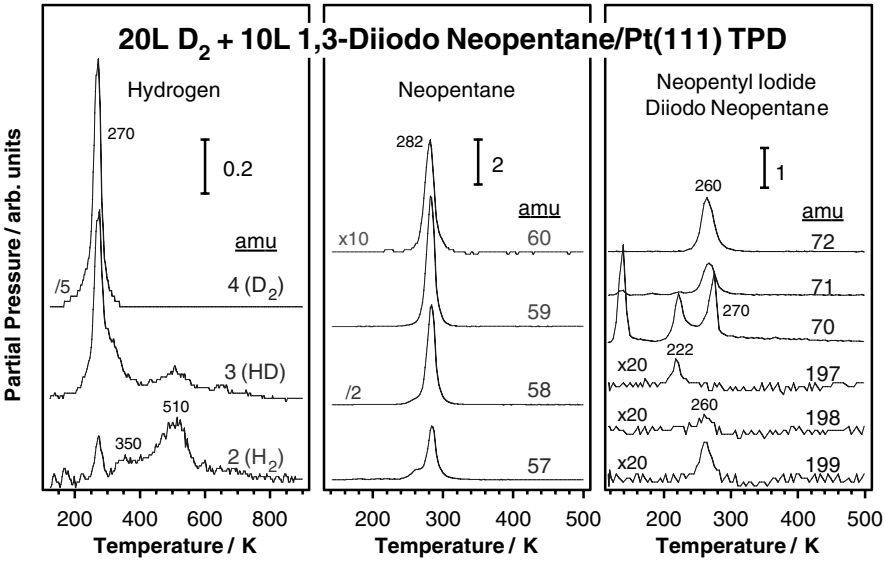

FIG. 5. Results from TPD experiments similar to those in Fig. 4 but with 1,3-diiodo neopentane. Neopentane production in this case occurs in a very narrow temperature range, about 281–283 K, and much less decomposition to surface carbon and hydrogen takes place.

In addition to decomposition, the diiodo compounds also undergo extensive hydrogenation (deuteriation) and H–D exchange when in the presence of surface deuterium. Direct deuteriation of the monoiodo surface intermediate produced after the first C–I bond scission is evident by the significant peaks at about 260 K in the 72 ($C_5H_{10}D^+$) and 199 ($C_5H_{10}DI^+$) amu traces (amounting to yields of 27 and 20% of the initial 1,1- and 1,3-diiodo neopentane adsorbed molecules, respectively). H–D exchange manifests itself by the nonzero signals seen in the high-temperature portion of the TPD trace for the 3 (HD) amu. Both exchange and hydrogenation reactions also lead to the formation of the neopentanes seen in the traces in the 57- to 60-amu range reported in the middle frame of Figs. 4 and 5. Broad features centered around 250 K are seen for the desorption of those products in the case of 1,1-diiodo neopentane, while much sharper peaks around 281–283 K are observed with the 1,3-isomer.

Small amounts (20 and 10%) of molecular desorption are seen in these cases as well, at around 215 and 222 K for the 1,1- and 1,3-diiodo neopentanes, respectively (see the 70-amu, $C_5H_{10}^+$, traces). The identity of the iodine-containing products was corroborated by following the signals for 197, 198, and 199 amu (right panels of Figs. 4 and 5): the 197-amu ($C_5H_{10}I^+$) fragment corresponds to the molecular diiodo neopentanes, while those at 198 ($C_5H_{11}I^+$) and 199 ($C_5H_{10}DI^+$) amu are the parent peaks for normal and monodeuteriated neopentyl iodide, respectively.

Neopentane production in these deuterium coadsorption experiments is extensive, amounting to 42 and 69% of the total 1,1- and 1,3-diiodo molecules adsorbed, respectively (about one-half and three-quarters of those that react). They correspond mostly to dideuterio neopentane, the result of direct deuteriation of the intermediates resulting from elimination of both iodine atoms. This is indicated by the large signals in the 59-amu ($C_4H_7D_2^+$) traces, especially in the case of 1,1-diiodo neopentane. Nevertheless, significant monodeuteriation as well as some H–D exchange is evident by the other traces in the middle panels of Figs. 4 and 5. In order to quantify the yields in these experiments, the data need to be analyzed via deconvolution of the cracking pattern of the neopentanes, accounting for the statistical distributions of the corresponding tertbutyl ($C_4X_9^+$) cations detected in the TPD (57–60 amu) in each neopentane isomer, and assuming either α or γ preferential H–D exchange (61). The yields resulting from such analysis are summarized in Fig. 6 together with the associated TPD peak maxima.

The quantitative data in Fig. 6 corroborate the main observations from Figs. 4 and 5. For one, it can be seen there that, indeed, the main isotopologue of neopentane produced in TPD experiments with either 1,1- or 1,3-diiodo neopentane and deuterium on Pt(111) is that containing two deuteriums. Concretely, the neopentane-d_2 yield in those experiments amounts to 49 and 57% of the total neopentane produced from 1,1- or 1,3-diiodo neopentane, respectively. Nevertheless, a significant fraction (25 and 31%) does incorporate only one deuterium, an observation that indicates that decomposition of the surface species, the source of normal H, competes with the hydrogenation steps in the relevant (200–300 K) temperature range. In fact, some normal neopentane is produced as well, as much as

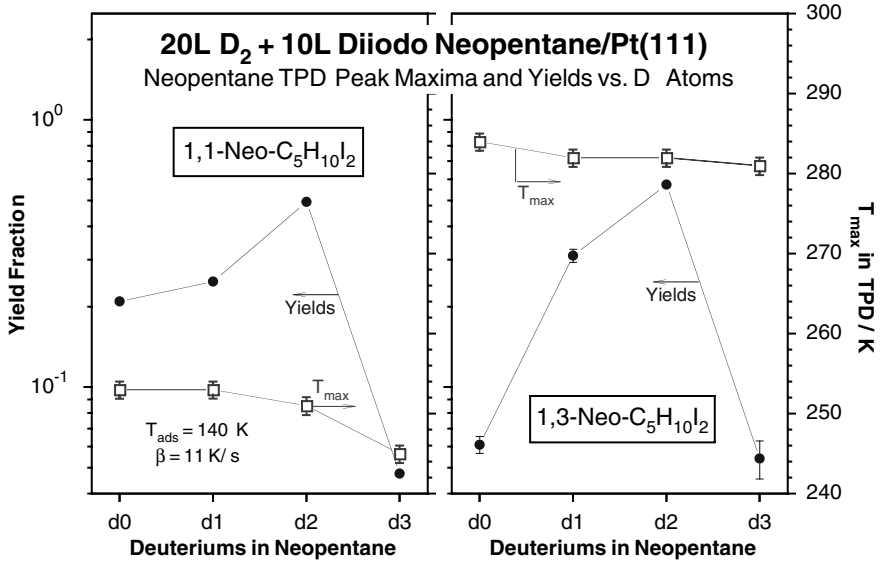

FIG. 6. Neopentane TPD peak maximum temperatures (open squares) and yields (filled circles) from experiments with deuterium and 1,1- (left) or 1,3- (right) diiodo neopentane on Pt(111), calculated from the data in Figs. 4 and 5 after appropriate calibrations. The main products are from straight hydrogenation or deuteriation of the neopentyl surface species, but some H–D exchange is manifested by the production of a small amount of neopentane-d_3. Notice also the measurable changes in temperature maxima for the different isotopologues.

21% in the case of the 1,1-diiodo compound (6% with 1,3-diiodo neopentane). The total amount of hydrogen incorporated in these normal and monodeuteriated neopentanes is much larger in the 1,1-diiodo case (67% of the total neopentane vs 43% for the 1,3-diiodo isomer), corroborating the more extensive decomposition there. Notice, however, that the higher extent of decomposition in the 1,1-diiodo case is accompanied by desorption of neopentane at lower temperatures (250 vs 280 K). H–D exchange is also manifested by the production of neopentane-d_3, about 5% in both cases. As already reported for neopentyl iodide, the hydrogenation and dehydrogenation steps in the diiodo neopentane conversion over Pt(111) display competing rates (more on this in the Discussion).

Finally, a small amount of normal neopentane is produced from 1,1-diiodo neopentane between 400 and 450 K (Fig. 4). This is likely the result of the hydrogenation of neopentylidyne, the intermediate formed on the surface above 300 K (see Discussion; see also (60)). An analogous reaction, the hydrogenation of propylidyne to propane on Pt(111), has been reported by us before (64). No high-temperature hydrogenation products were seen with 1,3-diiodo neopentane, though (Fig. 5).

3.3. Infrared Spectra of Molecular Species

The development of a further understanding of the chemistry of the surface species that form upon thermal activation of diiodo neopentanes on Pt(111) was aided by the use of infrared spectroscopy. We start this section by assigning the vibrational peaks observed for molecular 1,1- and 1,3-diiodo neopentanes to their corresponding vibrational normal coordinate modes. The appropriate spectra for the liquid compounds, those of the two diiodo neopentanes, as well as that of monoiodo neopentane, are presented in Fig. 7, and the assignments are summarized in Table 1.

The most noticeable and easiest to assign modes are those associated with the C–H stretching and deformation modes of the methyl groups. In the stretching region, the asymmetric modes are seen at 2963 and 2926 cm^{-1} in the spectra of 1,1-diiodo neopentane, and at 2950, 2935, and 2929 cm^{-1} in that of the 1,3-diiodo isomer. The corresponding symmetric stretches are at 2901, 2890, and 2865 cm^{-1}, and at 2902, 2873, and 2861 cm^{-1}, respectively. The methyl asymmetric deformation peaks are observed at 1472, 1458, and 1440 cm^{-1} in the first case, and at 1464 and 1462 cm^{-1} in the second. Finally, the methyl symmetric deformation (umbrella) mode can be identified at 1393 and 1365 cm^{-1}, and at 1382 and 1365 cm^{-1}, respectively. The multiple peaks observed for each of those modes are the result of splittings induced by the existence of either three (1,1-diiodo) or two (1,3-diiodo) methyl groups in the molecule.

A few infrared bands can be also unequivocally assigned to either the C–H group in 1,1-diiodo neopentane or the two methylene (CH_2) moieties in the 1,3-isomer. In the high-energy region of the spectra, the peak at 2971 cm^{-1} corresponds to the stretching of the C–H group in the first compound, and the bands at 2997 and 2964 cm^{-1} to the asymmetric and symmetric stretchings of the methylene in the second. The C–H in- and out-of-plane deformations in 1,1-diiodo neopentane can be located at 1221 and 1086 cm^{-1}, respectively, while the methylene symmetric (scissoring) modes in 1,3-diiodo neopentane show up at 1438 and 1413 cm^{-1}. These features are of particular importance here, because they allow us to distinguish among the different surface species containing methylene and CH moieties.

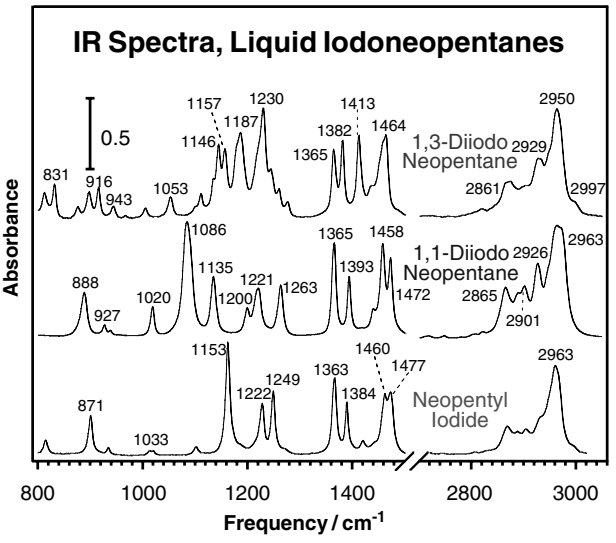

FIG. 7. Reflection–absorption infrared spectra (RAIRS) from liquid 1,1- and 1,3-diiodo neopentanes as well as from liquid neopentyl iodide. Our assignment of the different peaks in the spectra to specific normal vibrational modes is summarized in Table 1.

The remaining vibrational modes in the IR spectra are harder to identify, in part because of their high degree of mixing. Regardless, a number of the low-frequency peaks may be associated with C–C stretching and/or methyl rocking modes. We include the signals at 1263, 1200, 1135, 1020, 937, 927, and 888 cm^{-1} in 1,1-diiodo neopentane, and those at 1187, 1053, 1004, 985, 943, 916, 897, 831, and 813 cm^{-1} in 1,3-diiodo neopentane, into that group. Finally, a number of methylene twisting and waging modes can be seen for the second compound at 1277, 1253, 1242, 1230, 1157, 1146, and 1112 cm^{-1}.

3.4. Infrared Spectra of Surface Species from Thermal Activation of Diiodo Neopentanes

Figure 8 displays the RAIRS data for the surface species that form on Pt(111) upon exposure to 30 L of the diiodo neopentanes at 230 K. The spectrum for 50 L of neopentyl iodide is also included for comparison (60). This temperature was chosen as one likely to lead to the formation of the first surface intermediate expected from the thermal

TABLE 1

Vibrational Assignment of the Infrared Peaks for Liquid 1,1- and 1,3-Diiodo Neopentanes[a]

Vibrational mode[b]	1,1-Diiodo neopentane ($(CH_3)_3CCHI_2$)	Neopentyl iodide (60) ($(CH_3)_3CCH_2I$)	1,3-Diiodo neopentane ($(CH_3)_2C(CH_2I)_2$)	1,3-Dichloro neopentane (88) ($(CH_3)_2C(CH_2Cl)_2$)
$\nu_a(CH_2)$		2996 (sh)	2997 (sh)	2997 (w)
$\nu_s(CH_2)$			2964 (s)	2970 (m)
$\nu(CH)$	2971 (s)			
$\nu_a(CH_3)$	2963 (s), 2926 (m)	2960 (s), 2933 (sh)	2950 (sh), 2935 (m)	2954 (m), 2934 (vw)
$\nu_a(CH_3)$			2929 (m)	
$\nu_s(CH_3)$	2901 (m), 2890 (m)	2904 (m), 2888 (m)	2902 (w)	2894 (w)
$\nu_s(CH_3)$	2865 (m)	2869 (m)	2873 (w), 2861 (w)	2874 (m)
$\delta_a(CH_3)$	1472 (s), 1458 (s)	1472 (s), 1463 (s)	1464 (s), 1462 (sh)	1468 (vs)
$\delta_a(CH_3)$	1440 (m)	1445 (sh)		1452 (m-w)
$\delta(CH_2)$		1420 (w)	1438 (sh), 1413 (s)	1433 (s), 1429 (sh)
$\delta_s(CH_3)$	1393 (s), 1365 (s)	1389 (s), 1366 (s)	1382 (s), 1365 (s)	1386 (vs), 1368 (vs)
$\nu(C–C)/\rho(CH_3)$	1263 (m)	1249 (s)		
$\omega(CH_2)$		1227 (m)	1230 (s)	1296 (vs)
$\delta_{ip}(CH)$	1221 (m)			
$\omega(CH_2)/\tau(CH_2)$			1277 (w), 1253 (w)	1286 (sh), 1249 (m)
$\omega(CH_2)/\tau(CH_2)$			1242 (sh)	1238 (w)
$\nu(C–C)$	1200 (m), 1135 (m)	1218 (w)		
$\tau(CH_2)/\rho(CH_3)$		1102 (w)	1157 (m), 1146 (m)	1147 (m)
$\tau(CH_2)/\nu(C–C)$			1112 (w)	1108 (m)
$\nu(C–C)/\rho(CH_3)$			1187 (s)	1195 (m-s)
$\delta_{oop}(CH)$	1086 (s)			
$\rho(CH_3)$	1020 (m)	1020 (w), 1013 (w)	1053 (w), 1004 (vw)	1031 (vw), 1017 (m)
$\rho(CH_3)$		1013 (w)	985 (vw)	978 (m)
$\nu(C–C)$	937 (w)	934 (w)	943 (vw)	
$\rho(CH_3)/\nu(C–C)$	927 (w)		916 (w)	922 (m-s)
$\nu(C–C)$	888 (m)	901 (m)	897 (w)	910 (ms), 886 (m-s)
$\nu(C–C)$		814 (m)	831 (w), 813 (w)	857 (m-s)

[a] The spectra of neopentyl iodide and of 1,3-dichloro neopentane are also reported for reference. A rough indication of the peak intensities are indicated in parentheses: vs = very strong, s = strong, m = medium, w = weak, vw = very weak, sh = shoulder.

[b] ν = Stretching, δ = deformation, ρ = rocking, ω = wagging, τ = torsion, a = asymmetric, s = symmetric, ip = in plane, oop = out of plane.

conversion of the chemisorbed halo hydrocarbons based on TPD data for both neopentyl iodide and the diiodo compounds. The assignment of the peaks, discussed in more detail below, is also summarized in Table 2.

The IR spectra from the species formed with both diiodo neopentanes display many similarities. Again, the most straightforward modes to identify are those connected with the methyl groups. Methyl C–H asymmetric stretches are seen at 2958 and 2932 cm^{-1}, and at 2960 and 2940 cm^{-1}, in the spectra from 1,1- and 1,3-diiodo neopentane, respectively. The corresponding symmetric C–H stretching modes are located at 2911 and 2910 cm^{-1}, respectively. The methyl asymmetric deformations result in vibrations around 1475 and 1468 cm^{-1}, respectively, and the associated symmetric deformations are at 1400 and 1372 cm^{-1} and at 1383 and 1366 cm^{-1}, respectively.

In terms of specific modes for each compound, the species resulting from the 230 K adsorption of 1,1-diiodo neopentane on Pt(111) display clear IR peaks for the C–H stretching and in-plane deformation of a methylidene moiety (Pt_n = CHR) at 2972 and 1218 cm^{-1}, respectively, and for methyl rocking/C–C stretchings about 1256 and 974 cm^{-1}. In the case of the intermediate produced with 1,3-diiodo neopentane, the modes for the methylene (CH_2) moieties are seen at 2966 (symmetric stretch), 1225 (wag), and 1159 (twist) cm^{-1}, and C–C stretching and methyl rocking modes are visible at 1186 and 1048 cm^{-1}.

One thing to notice in both cases is the persistence of a good number of the peaks seen in the liquid compounds. This is particularly true in the 1,3-diiodo neopentane case, where no significant differences are observed in the C–H stretching and methyl deformation regions. The main changes there are in the relative intensities of some of the bands, specifically in the reduction of the CH_2 scissoring at 1413 cm^{-1} and the C–C stretching/methyl rocking at about 1187 cm^{-1}. This argues for the retention of most of the molecular structure, but for the adoption of a specific adsorption geometry (21, 65–68). The data here are consistent with the formation of a metallacyclic intermediate where the two iodine atoms are replaced by platinum atoms and where the planes of the methylene groups are parallel to the surface, perhaps because the plane of the ring is in a

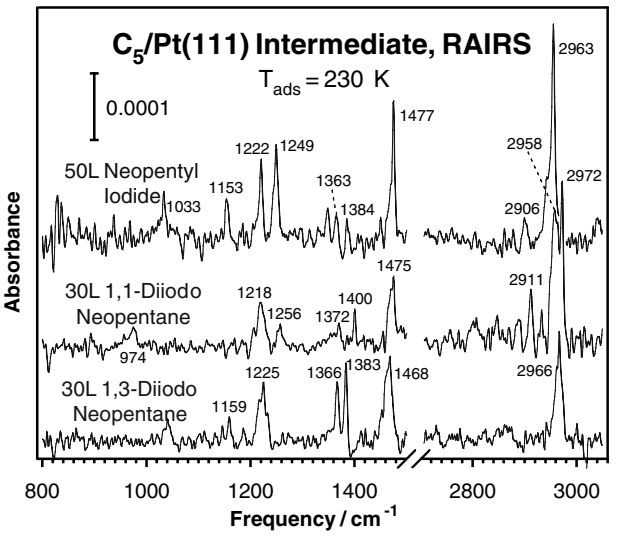

FIG. 8. RAIRS data from 30 L of 1,1- and 1,3-diiodo neopentanes and from 50 L of neopentane dosed at 230 K on a Pt(111) single-crystal surface. The assignment of the vibrational modes is provided in Table 2. It is our interpretation that the spectra for the 1,1- and 1,3-diiodo compounds correspond to 2,2-dimethyl propane-1-yl-3-ylidene and 2,2-dimethyl propane-1,3-diyl surface intermediates, respectively.

perpendicular configuration (a 2,2-dimethyl propane-1,3-diyl, Pt_n–$CH_2C(CH_3)_2CH_2$–Pt_n; see Fig. 10).

A few more changes are observed in the spectra for 1,1-diiodo neopentane. Many of the methyl C–H stretching and deformation modes become slightly displaced upon adsorption on Pt(111) at 230 K, and the asymmetric deformation at 1458 cm^{-1} disappears almost completely. Notice in particular the high frequencies and large split between the two methyl symmetric deformation modes (1400 and 1372 cm^{-1}). We interpret this as a consequence of further dehydrogenation of the neopentylidene, Pt_n=$CHC(CH_3)_3$, moiety. Also, the high intensity of the 1400-cm^{-1} peak relative to that at 1372 cm^{-1} argues for the methyl groups significantly tilted toward the surface. On the other hand, the persistence of the C–H group is clear, given the strong bands seen for its stretching and in-plane deformation at 2972 and 1218 cm^{-1}. Finally, there are some similarities between the spectrum from 1,1-diiodo neopentane at 230 K and that from neopentyl iodide at 170 K (which presumably corresponds to neopentyl surface species (60)). Of particular importance are the close positions in both cases for the methyl asymmetric (2958 vs 2952–2955 cm^{-1}) and symmetric (2911 vs 2904 cm^{-1}) stretches as well as for the methyl asymmetric (1475 vs 1472 cm^{-1}) and symmetric (1400, 1372 vs 1389, 1366 cm^{-1}) deformations. The higher frequencies seen in some of the bands in the data from the former compound could be again interpreted as the result of a more extensive dehydrogenated moiety. All this leads us to propose the formation of a α,α,γ-bonded dimethyl C_3-cyclic intermediate, perhaps 2,2-dimethyl propane-1-yl-3-ylidene, Pt_n=$CHC(CH_3)_2CH_2$–Pt_n (see Fig. 10).

3.5. Infrared Spectra of Surface Species from Thermal Activation of Iodo Neopentanes

One of the main objectives of this study was to understand the thermal chemistry of hydrocarbon surface species,

TABLE 2

Vibrational Assignment of the Infrared Peaks for 30 L of 1,1- and 1,3-Diiodo Neopentanes Dosed on Pt(111) at 230 K, as well as for Those of 50 L of a Number of Deuterium-Labeled Neopentyl Iodides Adsorbed at 235 K[a]

Vibrational mode[b]	1,1-Diiodo neopentane	1,3-Diiodo neopentane	Neopentyl iodide-d_0	Neopentyl iodide-d_2	Neopentyl iodide-d_9	Neopentyl iodide-d_{11}
$\nu(CX)$	2972 (s)					
$\nu_s(CX_2)$		2966 (s)				
$\nu_a(CX_3)$	2958 (s)	2960 (sh)	2963 (vs)	2965 (s)	2218 (s)	2217 (s)
$\nu_a(CX_3)$	2932 (w)	2940 (sh)	2950 (sh)	2948 (sh)		
$\nu_s(CX_3)$	2911 (m)	2910 (sh)	2906 (w)	2905 (vw)		
$\delta_a(CX_3)$	1475 (s)	1468 (s)	1477 (vs)	1478 (s)	1059 (s)	1061 (s)
$\delta_a(CX_3)$			1460 (sh)	1462 (m)	1050 (sh)	1052 (sh)
$\delta_s(CX_3)$	1400 (m)	1383 (s)	1384 (w)	1380 (w), 1395 (m)		
$\delta_s(CX_3)$	1372 (w)	1366 (m)	1363 (w)	1366 (m)		
ν(C–C)/$\rho(CX_3)$	1256 (w)		1249 (s)	1251 (s)		
$\delta_{ip}(CX)$	1218 (s)		1222 (s)	918 (m)	1218 (m)	903 (s)
$\omega(CX_2)$		1225 (s)	1222 (s)			1216 (w)
ν(C–C)		1186 (w)	1185 (w)		1192 (w)	1170 (w)
$\tau(CH_2)/\rho(CH_3)$		1159 (w)	1153 (m)	1150 (w)	1145 (w)	1140 (w)
$\rho(CX_3)$		1048 (w)	1033 (m)	1025 (w)		
$\rho(CX_3)$	974 (w)			970 (w)		
ν(C–C)			871 (vw)		822 (m)	

[a] A rough indication of the peak intensities are indicated in brackets: s = strong, m = medium, w = weak, vw = very weak, sh = shoulder. The *X* in the list of vibrational modes stands for either H or D.

[b] ν = Stretching, δ = deformation, ρ = rocking, ω = wagging, τ = torsion, *a* = asymmetric, *s* = symmetric, ip = in plane.

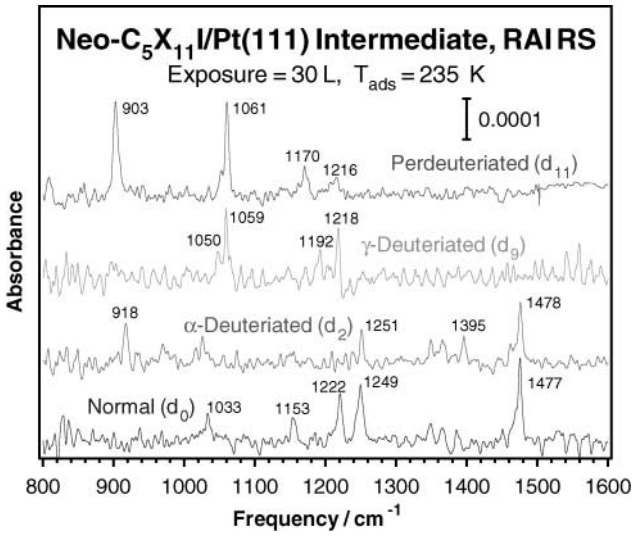

FIG. 9. RAIRS data recorded after adsorption of 30 L of neopentyl iodide-d_0, -α -d_2, -γ -d_9, and -d_{11} on Pt(111) at 235 K. The exact nature of the resulting surface intermediates depends on the regiospecificity of the deuterium labeling, as described in more detail in the text (see also (61)) but always involves a combination of neopentylidene, 2,2-dimethyl propane-1,3-diyl, and 2,2-dimethyl propane-1-yl-3-ylidene. The vibrational assignment is provided in Table 2.

in particular in connection with the regioselectivity of dehydrogenation steps. To that goal, experiments were also carried out with a number of isotope-substituted iodo neopentanes, the precursor of neopentyl surface species (60). Four different isotopologues were used here, namely normal (not deuterium substituted) and α-, γ-, and per-deuteriated neopentyl iodides (neopentyl iodide-d_0, -d_2, -d_9, and -d_{11}, respectively). The infrared spectra obtained after 30-L doses of those compounds on Pt(111) at 235 K are presented in Fig. 9, and the corresponding vibrational mode assignments are summarized in Table 2.

To begin with, it may be worthwhile to contrast the spectrum from the nondeuteriated case to those obtained with the diiodo compounds (Fig. 8). A few features of the former can be associated with vibrations seen in the latter. For instance, the C–H stretches at 2963 and 2906 cm^{-1} (methyl asymmetric and symmetric modes, respectively) of the species from the monoiodo compound can be seen at 2958 and 2911 cm^{-1} in the data for 1,1-diiodo neopentane adsorbed at 230 K (at 2963 and 2901 cm^{-1} for the liquid), and the methyl asymmetric deformation observed at 1477 matches that at 1475 cm^{-1}. The C–C stretching/methyl rocking at 1249 cm^{-1} for iodo neopentane adsorbed at 235 K shows up at about 1256 cm^{-1} in the trace of the 1,1-diiodo/230 K case. At least part of the intensity of the 1222-cm^{-1} peak could be due to the same in-plane C–H deformation as that at 1218 cm^{-1} in 1,1-diiodo neopentane. Given the higher frequencies of the methyl asymmetric modes and the lower energies of the symmetric ones in the species from the monoiodo neopentane, and also the better match of some of the peaks to those in the spectrum of liquid 1,1-diiodo neopentane, we suggest that iodo neopentane adsorption on Pt(111) at 235 K may lead to the formation of neopentylidene, $Pt_n{=}CHC(CH_3)_3$ (Fig. 10).

The spectra from monoiodo neopentane thermal activation also show some additional features common to the vibrational data for the intermediate obtained with 1,3-diiodo neopentane. For instance, although weak, the modes at 1384 and 1363 cm^{-1} could be connected to the methyl umbrella modes at 1383 and 1366 cm^{-1} in the metallacyclic species produced with the 1,3-diiodo precursor. The peak at 1222 cm^{-1} could have a component from the methylene wagging seen at about 1225 cm^{-1} in the latter species. Perhaps more striking is the similarity of both spectra below 1200 cm^{-1}, in particular with respect to the peaks at 1185, 1153, and 1033 cm^{-1}, seen at 1186, 1159, and 1048 cm^{-1} with 1,3-diiodo neopentane (the C–C stretching, methylene twisting, and methyl rocking, respectively). This is particularly significant because almost no features are observed in that region of the spectra of iodo neopentane adsorbed at 170 K (60). We contend that thermal activation of neopentyl iodide on Pt(111) at 235 K also leads to the formation of a 2,2-dimethyl propane-1,3-diyl intermediate (Fig. 10).

The previous assignment is supported by the RAIRS data obtained with the deuterium-labeled neopentyl iodide compounds (Fig. 9). Besides the obvious redshifts in the methyl modes with deuterium substitutions (the main reason for the differences between the spectra from neopentyl iodide-d_0 and neopentyl iodide-d_2 on one side and neopentyl iodide-d_9 and neopentyl iodide-d_{11} on the other), other smaller changes can be used to support the conclusions of our previous discussion. One surprising observation is the fact that the trace for the α-substituted species displays many of the features (the 2905- and 1251-cm^{-1} peaks) associated with neopentylidene. This is not expected, since neopentylidene is produced via α-hydride elimination from neopentyl moieties, and that reaction is slowed down by the substitution of hydrogens for deuteriums in the α carbon (61). It is quite possible that although γ-H elimination is favored in that case, the concentration of the resulting metallacyclic intermediate on the surface is kept low because of the reversible nature of such a reaction. In fact, the peaks for the methyl symmetric vibrations at 1380 and 1366 cm^{-1} are more in tune with those of the metallacycle made with 1,3-diiodo neopentane, and the mode at 918 cm^{-1} could be associated with the deuteriated methylene wagging mode of that species (also seen at 903 cm^{-1} in the case of the perdeuterio neopentane; alternatively, they could correspond to a C–D deformation). The high frequency of one of the methyl symmetric deformation modes (at 1395 cm^{-1}) suggests the formation of some of the same α,α,γ-bonded intermediate seen with 1,1-diiodo neopentane. In summary, the thermal activation of neopentyl iodide-α-d_2 on Pt(111) at 230 K appears to lead to the formation of a mixture

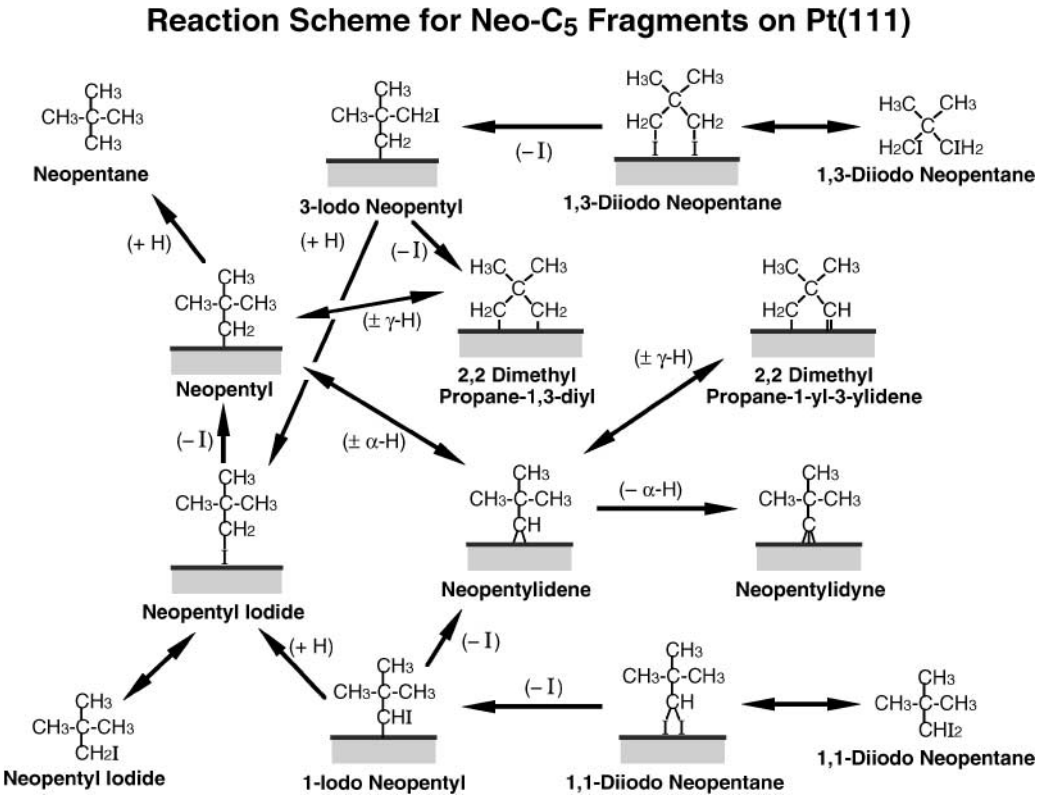

FIG. 10. Schematic representation of the surface reactions observed during the thermal activation of neopentyl iodide and of 1,1- and 1,3-diiodo neopentanes on Pt(111) surfaces.

of neopentylidene, 2,2-dimethyl propane-1,3-diyl, and 2,2-dimethyl propane-1-yl-3-ylidene.

Activation of neopentyl iodide-d_9 at 230 K is believed to produce mainly neopentylidene surface species. The methyl stretching and deformation modes, now shifted to lower frequencies because of the isotopic substitution, are consistent with this assessment. Also supporting that conclusion is the intense band at 1218 cm^{-1}, associated with the in-plane deformation of the C–H moiety. Finally, the IR spectrum from the perdeuteriated species displays the prominent peaks at 1061 and 903 cm^{-1} corresponding to the methyl asymmetric and in-plane C–D deformation in per-deuterio neopentylidene.

4. DISCUSSION

The data reported here contribute to our development of a better understanding of the chemistry of hydrocarbon species on transition metal surfaces. In previous work we characterized the reactivity of neopentyl groups on Ni(100) (39, 58) and Pt(111) (59–61) surfaces. Neopentyl moieties were chosen as the target of our investigation because of their lack of hydrogen atoms at the β position, which render them unreactive toward their decomposition via the much preferred β-hydride elimination step (2, 4, 51). On nickel surfaces, it was determined that removal of hydrogen atoms from such neopentyl groups takes place preferentially from the α-carbon (39, 58). The first dehydrogenation step in the neopentyl moieties on Ni(100) occurs at quite low temperatures, perhaps below 150 K, but further decomposition of the resulting neopentylidene, $Ni_n{=}CHC(CH_3)_3$, intermediate is only triggered above 350 K and goes through a complex transition state, where both α- and γ-hydrogens are removed while the C_α–C_β bond is broken and isobutene is produced.

The surface chemistry of neopentyls on platinum is somewhat more involved. There, elimination of hydrogen atoms from the α and γ positions proceeds at comparable rates, and the decomposition pathway can change after selective isotopic substitution: a kinetic isotope effect controls the relative rates (59, 61). To complement our studies on the surface chemistry of neopentyl groups (prepared via the thermal activation of adsorbed neopentyl iodide), the reactivity of the intermediates expected from those steps, neopentylidene, $Pt_n{=}CHC(CH_3)_3$, and 2,2-dimethyl propane-1,3-diyl, $Pt_n{-}CH_2C(CH_3)_2CH_2{-}Pt_n$, was probed here via the use of 1,1- and 1,3-diiodo neopentanes, respectively.

As in many other cases (1, 10, 12), the C–I bonds in 1,1- and 1,3-diiodo neopentanes proved easy to activate thermally on the Pt(111) surface. Perhaps the best evidence for

that is the production of both neopentyl iodide and neopentane seen in the TPD experiments with the two compounds. In addition, it is also clear that the scission of the two C–I bonds takes place sequentially, otherwise there could not be any formation of neopentyl iodide. Notice in particular the desorption of monodeuteriated neopentyl iodide in the experiments with coadsorbed deuterium (shown by the peaks in the 199-amu trace of the TPD data in Figs. 4 and 5). The kinetics of neopentane and neopentyl iodide desorption yield TPD peaks with different shapes, the production of the former trailing that of the latter (Figs. 1 and 2): in the case of 1,1-diiodo neopentane, the peak maxima for neopentane and neopentyl iodide are seen at 255 and 235 K, respectively, while with 1,3-diiodo neopentane those features are seen at about 285 and 265 K. The kinetics of desorption of those compounds are likely to be limited by the decomposition of some of the surface species, the origin of the needed hydrogen for the hydrogenation steps, although the detection of the neopentyl iodide could be also controlled by its own molecular desorption from the monolayer, which occurs at about 240 K (60). Tellingly, the coadsorption of deuterium does not shift the neopentyl iodide TPD peaks obtained with the diiodo compounds in any significant way.

Once the C–I bonds in the adsorbed diiodo neopentanes are broken, the resulting hydrocarbon species appear to be fairly stable on the surface. No hydrogen desorbs below 400 K in the TPD of either 1,1- or 1,3-diiodo neopentanes on clean Pt(111), suggesting that the resulting surface moieties retain their carbon skeleton and their hydrogen atoms through a wide range of temperatures. This appears to be truer for 1,3-diiodo neopentane, which decomposes to a much lesser extent (significantly less hydrogen is produced in the TPD experiments; compare the data in Figs. 1 and 2), although some normal hydrogen does leave the surface above 300 K in the case where deuterium is predosed on the surface (Fig. 5). With 1,1-diiodo neopentane, a large amount of hydrogen is seen on the clean platinum, but only above 500 K (Fig. 1). On the other hand, a significant HD signal is detected in the 255 K peak in the experiments with deuterium (Fig. 4), indicating earlier decomposition here too; only what the hydrogen produced at low temperatures on the clean surface is consumed by the production of neopentane. In any case, it can be concluded that both 1,1- and 1,3-diiodo neopentanes decompose below 230 K on Pt(111) via the sequential scission of their C–I bonds, and that such reactions produce a number of complex hydrocarbon surface species with most of the original carbon backbone until reaching temperatures above 300 K.

The next step in our discussion is to identify the nature of the intermediates produced by thermal activation of 1,1- and 1,3-diiodo neopentanes on the Pt(111) surface. The expectation, based on simple chemical intuition, is for the formation of neopentylidene and 2,2-dimethyl propane-1,3-diyl, respectively (Fig. 10). The infrared spectroscopy data reported in this paper is in great part supportive of that hypothesis. The vibrational assignments for the 1,3-diiodo case in particular are fairly straightforward, since the IR trace for the intermediate formed at 230 K closely resembles that of liquid 1,3-diiodo neopentane, indicating minimal structural rearrangement. Only changes in the peak relative intensities are obvious in that comparison, variations that can be explained by a particular adsorption geometry with the plane of the carbon cyclic backbone perpendicular to the surface. In analogy with organometallic compounds (4, 69), we assume that a platinacyclobutane ring forms where the two end carbons are coordinated to the same platinum surface atom. However, we have no direct evidence to support this claim, and coordination could very well take place via two separate surface centers instead.

The case of the Pt(111) surface chemistry of 1,1-diiodo neopentane is a bit more complicated. There, the significant differences observed in the infrared spectra obtained upon dosing at 110 versus 230 K led us to conclude that some dehydrogenation takes place by the latter temperature. Our data are consistent with the formation of a α,α,γ-bonded dimethyl C_3-cyclic intermediate, presumably 2,2-dimethyl propane-1-yl-3-ylidene, $Pt_n{=}CHC(CH_3)_2CH_2{-}Pt_n$. We suggest that that species may form via γ-hydride elimination from neopentylidene, an idea supported by the detection of vibrational features associated with the neopentylidene moiety during the activation of neopentyl iodide on Pt(111) (Fig. 8; see also (60)). It is clear that surface neopentylidene is fairly reactive and converts easily to either a cyclic intermediate or neopentylidene (60). On the other hand, rehydrogenation of the α, α, γ-bonded cyclic species to neopentylidene is also facile (61), so the end product in all this chemistry at 300 K is neopentylidyne (60).

We are left with trying to understand the relative rates for the different hydrogenation and dehydrogenation steps involved in the interconversion of the several surface species observed in this C_5 chemistry on Pt(111). Deuterium labeling, either regioselectively on neopentyl groups or via coadsorption with D_2, helps in this endeavor. We have already determined that the rate of α-H elimination from neopentyl surface groups on Pt(111) is about six times faster than dehydrogenation from the γ position (61). However, this difference in rate per C–H bond is compensated in part by the existence of more hydrogens in the γ versus the α position in neopentyl groups (9 vs 2); the observed overall dehydrogenation rates from both positions are approximately the same. A significant normal kinetic isotope effect also plays a dominant role in determining the selectivity in reactions with deuterium-labeled compounds, the conversion with the light hydrogen being approximately eight times faster than that with deuterium (61).

The TPD data in Figs. 1–5 clearly indicate that the intermediates that form from 1,1-diiodo neopentane are more

prone to total decomposition than those from 1,3-diiodo neopentane activation. This is easy to understand based on the nature of the resulting surface intermediates (Fig. 10). Specifically, the neopentylidene that forms initially during the conversion of the former compound can be easily dehydrogenated further at the α position to yield neopentylidyne, $Pt_n{\equiv}CC(CH_3)_3$. Indeed, neopentylidyne was seen to form when adsorbing neopentyl iodide on Pt(111) above 270 K (60). Also, it has been previously reported that ethylidene, prepared by activation of 1,1-diiodo ethane, can dehydrogenate to ethylidyne on Pt(111) at temperatures as low as 150 K (31). Alkylidynes are particularly stable species (20, 62, 70–76) difficult to rehydrogenate to other species (49, 50, 72, 77–79) and, therefore, can be considered dead ends in reaction schemes of surface hydrocarbon species at low temperatures (below room temperature). The infrared spectra reported here for the species formed by adsorption of 1,1-diiodo neopentane at 230 K are consistent with a metallacyclic moiety (from γ-H elimination from neopentylidene), but such an intermediate may very well hydrogenate back to neopentylidene before undergoing α-H elimination to neopentylidyne.

Much less extensive dehydrogenation is seen in the case of 1,3-diiodo neopentane on Pt(111). In that case, the first expected intermediate, 2,2-dimethyl propane-1,3-diyl, can be easily isolated on the surface at 230 K (Fig. 8 and Table 2). Previous surface chemistry work has indicated that metallacycle surface species tend to decompose via β-H elimination to yield allylic moieties (38, 40, 41, 43), but that pathway is blocked here by the methyl groups bonded to the β-carbon. Alternatively, the cyclic intermediate can undergo C–C coupling to generate cyclopropane, a reaction reported on silver (23) and, more surprisingly, on nickel (41, 42). Nevertheless, carbon coupling has yet to be observed in surface-science experiments with platinum (43) and was not seen here either. That leaves us with two other options to consider. On the one hand, the 2,2-dimethyl propane-1,3-diyl could dehydrogenate at the α position to generate 2,2-dimethyl propane-1-yl-3-ylidene. That reaction seems unlikely, however, because of the steric constrains imposed by the four-member ring structure, and because it could be easily followed by rehydrogenation to neopentylidene and dehydrogenation to neopentylidyne (see above). Instead, we contend that 2,2-dimethyl propane-1,3-diyl mostly rehydrogenates directly back to neopentyl surface species (Fig. 10).

A number of observations can be explained by the model developed in the previous paragraphs. First, it should be remembered that no cyclic intermediate was detected at 230 K with neopentyl iodide-α-d_2 (Fig. 9; see also (60)), even though γ-H elimination is favored there. It would seem that the reversible rehydrogenation of the cyclic intermediate, favored because of its relative stability toward further dehydrogenation, precludes its isolation in that case. Ultimately, all neopentyl iodide isotopologues lead to the formation of the same neopentylidyne intermediate at 270 K (60). On the other hand, several pieces of evidence suggest that H–D exchange in adsorbed neopentyl species is easier at the α position (61). For instance, the extent of the H–D exchange (per hydrogen atom) in neopentyl-α-d_2 at the α-carbon amounts to 8.5% of the total neopentane produced, while that at the γ-C in the γ-labeled compound comes up to be only 2.5% (61). Also, particularly large amounts of neopentane-d_3 and -d_9 production are seen in experiments with $D_2 + C_5H_{11}I$ and $H_2 + C_5D_{11}I$, respectively, suggesting again extensive exchange at the α-carbon (that methyl being fully exchanged). Overall, it could be concluded that α-dehydrogenation may be more reversible than γ-elimination, but that neopentylidene eventually dehydrogenates to the stable (hard to hydrogenate) neopentylidyne, while the cyclic intermediate is so stable that it can only rehydrogenate back to neopentyl.

As mentioned in the introduction, the chemistry of neopentyl and diiodo neopentanes on Pt(111) elucidated here can be directly incorporated into the mechanism of catalytic hydrocarbon reforming. Most likely, the regioselectivity of the dehydrogenation steps from the early surface intermediates controls the ultimate product selectivity of that process (8, 9, 55, 56). Hydrogen elimination at the α position has been traditionally associated with hydrogenolysis reactions (52–54), and that is what has been seen on nickel and iron surfaces, on both films (80) and single crystals (58, 81). On the other hand, dehydrogenation at the γ position (with the resulting metallacycle formation) is believed to be required during isomerization reactions. Three basic steps have been proposed to explain these reactions: (i) direct isomerization via an α,α,γ-tricoordinated bridged species (82); (ii) intermediate isomerization of that tricoordinated metallacycle to a monocoordinated cyclopentyl species (83); and (iii) methyl transfer via a cyclopentanelike intermediate, the same as in the bond-shift mechanism in carbonium ions (84, 85). Explicit evidence for the first step has been reported here. Finally, the catalytic H–D exchange of neopentane has been shown to be limited mostly to one methyl group, and to yield mainly neopentane-d_1 and neopentane-d_3 on both nickel (80, 86) and platinum films (87). The most accepted mechanism for this reaction involves the initial activation of neopentane to neopentyl on the surface followed by two competing pathways, a reductive elimination with surface deuterium to neopentane-d_1, and a fast interconversion to an α,α-diadsorbed species (neopentylidene) followed by a slower hydrogenation to neopentane-d_3. These ideas are consistent with the results of our work.

5. CONCLUSIONS

The thermal chemistry of 1,1- and 1,3-diiodo neopentanes on Pt(111) was studied by TPD and RAIRS. As is the case of most iodo compounds, those adsorbates decompose

via the sequential scission of their two C–I bonds. The first reaction is likely to lead to the formation of monoiodo neopentyl intermediates, as indicated indirectly by the detection of neopentyl iodide in the TPD data, and the second to produce new dicoordinated surface species. In the case of 1,3-diiodo neopentane, the expected 2,2-dimethyl propane-1,3-diyl metallacyclic intermediate was isolated at 230 K. In fact, RAIRS data indicated an adsorption geometry with the four-member ring close to perpendicular to the surface. With 1,1-diiodo neopentane, activation at 230 K was shown to lead to the formation of 2,2-dimethyl propane-1-yl-3-ylidene, presumably via the removal of a γ-hydrogen from neopentylidene. Neopentylidene was identified on the platinum surface after activation of neopentyl iodide, and significant amounts of neopentane from hydrogenation of that species were seen in TPD experiments with the 1,1-diiodo compound (as well as with the 1,3-diiodo counterpart).

It was also determined that coadsorption of the diiodo neopentanes with deuterium mostly enhances hydrogenation (deuteriation) of the surface species, but it also leads to a minor amount (about 5%) of H–D exchange. Similar chemistry was observed with neopentyl iodide, although regiospecific deuterium substitution in that case alters the selectivity of the dehydrogenation pathways. Evidence for the formation of all neopentylidene, 2,2-dimethyl propane-1,3-diyl, and 2,2-dimethyl propane-1-yl-3-ylidene was obtained there. We believe that these are crucial intermediates in the surface chemistry of catalytic reforming processes. The reactions identified in our study are summarized in the scheme presented in Fig. 10.

ACKNOWLEDGMENT

Financial support for this project was provided by the National Science Foundation under Grant CHE-9819652.

REFERENCES

1. Zaera, F., *Surf. Sci.* **219**, 453 (1989).
2. Zaera, F., *Acc. Chem. Res.* **25**, 260 (1992).
3. Zaera, F., *J. Mol. Catal.* **86**, 221 (1994).
4. Zaera, F., *Chem. Rev.* **95**, 2651 (1995).
5. Tjandra, S., and Zaera, F., *J. Am. Chem. Soc.* **117**, 9749 (1995).
6. Zaera, F., *Isr. J. Chem.* **38**, 293 (1998).
7. Jenks, C. J., Bent, B. E., and Zaera, F., *J. Phys. Chem. B* **104**, 3017 (2000).
8. Zaera, F., *Prog. Surf. Sci.* **69**, 1 (2001).
9. Zaera, F., *J. Phys. Chem. B* **106**, 4043 (2002).
10. Tjandra, S., and Zaera, F., *J. Vac. Sci. Technol. A* **10**, 404 (1992).
11. Bent, B. E., Nuzzo, R. G., Zegarski, B. R., and Dubois, L. H., *J. Am. Chem. Soc.* **113**, 1137 (1991).
12. Lin, J.-L., Teplyakov, A. V., and Bent, B. E., *J. Phys. Chem.* **100**, 10721 (1996).
13. White, J. M., *J. Mol. Catal. A* **131**, 71 (1998).
14. Zaera, F., *J. Phys. Chem.* **94**, 8350 (1990).
15. Zaera, F., and Hoffmann, H., *J. Phys. Chem.* **95**, 6297 (1991).
16. Jenks, C. J., Bent, B. E., Bernstein, N., and Zaera, F., *J. Am. Chem. Soc.* **115**, 308 (1993).
17. Tjandra, S., and Zaera, F., *Surf. Sci.* **289**, 255 (1993).
18. Tjandra, S., and Zaera, F., *Langmuir* **10**, 2640 (1994).
19. Gleason, N. R., and Zaera, F., *J. Catal.* **169**, 365 (1997).
20. Chrysostomou, D., French, C., and Zaera, F., *Catal. Lett.* **69**, 117 (2000).
21. Jenks, C. J., Bent, B. E., Bernstein, N., and Zaera, F., *J. Phys. Chem. B* **104**, 3008 (2000).
22. Zhou, Y., Henderson, M. A., Feng, W. M., and White, J. M., *Surf. Sci.* **224**, 386 (1989).
23. Zhou, X.-L., and White, J. M., *J. Phys. Chem.* **95**, 5575 (1991).
24. Bent, B. E., Nuzzo, R. G., Zegarski, B. R., and Dubois, L. H., *J. Am. Chem. Soc.* **113**, 1143 (1991).
25. Chiang, C.-M., Wentzlaff, T. H., and Bent, B. E., *J. Phys. Chem.*. **96**, 1836 (1992).
26. Yang, M. X., Jo, S. K., Paul, A., Avila, L., Bent, B. E., and Nishikida, K., *Surf. Sci.* **325**, 102 (1995).
27. Solymosi, F., and Révész, K., *J. Am. Chem. Soc.* **113**, 9145 (1991).
28. Solymosi, F., Bugyi, L., and Oszkó, A., *Langmuir* **12**, 4145 (1996).
29. Tjandra, S., and Zaera, F., *J. Catal.* **144**, 361 (1993).
30. Solymosi, F., *Catal. Today* **28**, 193 (1996).
31. Janssens, T. V. W., and Zaera, F., *J. Phys. Chem.* **100**, 14118 (1996).
32. Wu, G., Kaltchev, M., and Tysoe, W. T., *Surf. Rev. Lett.* **6**, 13 (1999).
33. Liu, Z.-M., Zhou, X.-L., Buchanan, D. A., Kiss, J., and White, J. M., *J. Am. Chem. Soc.* **114**, 2031 (1992).
34. Zaera, F., and Bernstein, N., *J. Am. Chem. Soc.* **116**, 4881 (1994).
35. Tjandra, S., and Zaera, F., *J. Catal.* **164**, 82 (1996).
36. Ihm, H., and White, J. M., *Langmuir* **14**, 1398 (1998).
37. Celio, H., Smith, K. C., and White, J. M., *J. Am. Chem. Soc.* **121**, 10422 (1999).
38. Chrysostomou, D., and Zaera, F., *J. Phys. Chem. B* **105**, 1003 (2001).
39. Zaera, F., Tjandra, S., and Janssens, T. V. W., *Langmuir* **14**, 1320 (1998).
40. Scoggins, T. B., and White, J. M., *J. Phys. Chem. B* **103**, 9663 (1999).
41. Tjandra, S., and Zaera, F., *J. Phys. Chem. B* **101**, 1006 (1997).
42. Tjandra, S., and Zaera, F., *J. Phys. Chem. A* **103**, 2312 (1999).
43. Chrysostomou, D., Chou, A., and Zaera, F., *J. Phys. Chem. B* **105**, 5968 (2001).
44. Jones, G. S., Mavrikakis, M., Barteau, M. A., and Vohs, J. M., *J. Am. Chem. Soc.* **120**, 3196 (1998).
45. Wu, G., Stacchiola, D., Kaltchev, M., and Tysoe, W. T., *Surf. Sci.* **463**, 81 (2000).
46. Bond, G. C., "Catalysis by Metals." Academic, London, 1962.
47. Gates, B. C., Katzer, J. R., and Schuit, G. C. A., "Chemistry of Catalytic Processes." McGraw–Hill, New York, 1979.
48. Somorjai, G. A., and Zaera, F., *J. Phys. Chem.* **86**, 3070 (1982).
49. Zaera, F., and Somorjai, G. A., *in* "Hydrogen Effects in Catalysis: Fundamentals and Practical Applications" (Z. Paál and P. G. Menon, Eds.), p. 425. Dekker, New York, 1988.
50. Zaera, F., *Langmuir* **12**, 88 (1996).
51. Zaera, F., *J. Am. Chem. Soc.* **111**, 8744 (1989).
52. Kemball, C., *Catal. Rev.* **5**, 33 (1971).
53. Anderson, J. R., *Adv. Catal.* **23**, 1 (1973).
54. Gault, F. G., *Adv. Catal.* **30**, 1 (1981).
55. Zaera, F., *Appl. Catal.* **229**, 75 (2002).
56. Zaera, F., *Mol. Phys.*, In press.
57. Zaera, F., and Tjandra, S., *J. Am. Chem. Soc.* **115**, 5851 (1993).
58. Zaera, F., and Tjandra, S., *J. Am. Chem. Soc.* **118**, 12738 (1996).
59. Janssens, T. V. W., Jin, G., and Zaera, F., *J. Am. Chem. Soc.* **119**, 1169 (1997).
60. Janssens, T. V. W., and Zaera, F., *Surf. Sci.* **501**, 1 (2002).
61. Janssens, T. V. W., and Zaera, F., *Surf. Sci.* **501**, 16 (2002).
62. Hoffmann, H., Griffiths, P. R., and Zaera, F., *Surf. Sci.* **262**, 141 (1992).
63. Rydon, H. N., *Org. Syn.* **51**, 44 (1971).
64. Zaera, F., and Chrysostomou, D., *Surf. Sci.* **457**, 89 (2000).
65. Greenler, R. G., *J. Chem. Phys.* **44**, 310 (1966).
66. Zaera, F., Hoffmann, H., and Griffiths, P. R., *J. Electron Spectrosc. Relat. Phenom.* **54/55**, 705 (1990).

67. Parikh, A. N., and Allara, D. L., *J. Chem. Phys.* **96**, 927 (1992).
68. Zaera, F., *in* "Encyclopedia of Chemical Physics and Physical Chemistry" (J. H. Moore and N. D. Spencer, Eds.), p. 1563. IOP, Philadelphia, 2001.
69. Collman, J. P., Hegedus, L. S., Norton, J. R., and Finke, R. G., "Principles and Applications of Organotransition Metal Chemistry." University Science Books, Mill Valley, CA, 1987.
70. Kesmodel, L. L., Dubois, L. H., and Somorjai, G. A., *Chem. Phys. Lett.* **56**, 267 (1978).
71. Skinner, P., Howard, M. W., Oxton, I. A., Kettle, S. F. A., Powell, D. B., and Sheppard, N., *J. Chem. Soc. Faraday Trans. 2* **77**, 1203 (1981).
72. Zaera, F., Janssens, T. V. W., and Öfner, H., *Surf. Sci.* **368**, 371 (1996).
73. Zaera, F., and Chrysostomou, D., *Surf. Sci.* **457**, 71 (2000).
74. Koestner, R. J., Frost, J. C., Stair, P. C., Van Hove, M. A., and Somorjai, G. A., *Surf. Sci.* **116**, 85 (1982).
75. Avery, N. R., and Sheppard, N., *Proc. R. Soc. London Ser. A* **405**, 1 (1986).
76. Chesters, M. A., De La Cruz, C., Gardner, P., McCash, E. M., Pudney, P., Shahid, G., and Sheppard, N., *J. Chem. Soc. Faraday Trans.* **86**, 2757 (1990).
77. Davis, S. M., Zaera, F., Gordon, B., and Somorjai, G. A., *J. Catal.* **92**, 240 (1985).
78. Wieckowski, A., Rosasco, S. D., Salaita, G. N., Hubbard, A., Bent, B. E., Zaera, F., Godbey, D., and Somorjai, G. A., *J. Am. Chem. Soc.* **107**, 5910 (1985).
79. Loaiza, A., Xu, M., and Zaera, F., *J. Catal.* **159**, 127 (1996).
80. Kemball, C., and Kempling, J. C., *Proc. R. Soc. London Ser. A* **329**, 391 (1972).
81. Meagher, K. K., Bocarsly, A. B., Bernasek, S. L., and Ramanarayanan, T. A., *J. Phys. Chem. B* **104**, 3320 (2000).
82. Anderson, J. R., and Avery, N. R., *J. Catal.* **5**, 446 (1966).
83. Garin, F., and Gault, F. G., *J. Am. Chem. Soc.* **97**, 4466 (1975).
84. McKervey, M. A., Rooney, J. J., and Samman, N. G., *J. Catal.* **30**, 330 (1973).
85. Karpinski, Z., and Guczi, L., *J. Chem. Soc. Chem. Commun.* 563 (1977).
86. Kemball, C., *Trans. Faraday Soc.* **50**, 1344 (1954).
87. Brown, R., Kemball, C., Oliver, J. A., and Sadler, I. H., *J. Chem. Res. Miniprint* 3201 (1985).
88. Powell, D. L., Klaeboe, P., and Saebø, K., *J. Mol. Struct.* **98**, 55 (1983).